Electronic Supplementary Material (ESI) for Journal of Materials Chemistry A.

Supporting Information

O Species Decorated Graphene Shell Encapsulating Iridium-Nickel alloy as Efficient Electrocatalysts towards Hydrogen Evolution Reaction

Shipeng Gong[1], Changlai Wang[1], Peng Jiang[1], Kang Yang[1], Jian Lu[1], Minxue Huang[1], Shi Chen[1], Junzheng Wang[1], and Qianwang Chen[1,2*]

Experimental section

Synthesis of Ir-doped Ni-btc precursor and IrNi@OC: Typically, 128 mg $Ni(NO_3)_2$•$6H_2O$ and 51 mg trimesic acid were dissolved in 45 mL methanol. After stirring for 10 min, 1 mL H_2IrCl_6 (10 mg/mL) was added to obtain a homogeneous solution. Then after continuous stirring for 1 h, the mixed solution was sealed in a Teflon-lined 60 mL autoclave and heated at 150℃ for 12 h. The precipitate was collected and washed three times with methanol, and then dried in oven at 60℃.

The prepared precursor was annealed at 430 to 700℃ for 8 h under nitrogen flow with a heating rate of 5℃ min^{-1}. The obtained black powder was named as IrNi@OC-T. And Ni@OC-430 was prepared using the same method without adding H_2IrCl_6.

Synthesis of IrNi: we prepared IrNi alloy based on the previous work reported by Shaojun Guo (*Adv. Mater*. 2017, 1703798). In brief, 20mg $Ni(NO_3)_2$, 2 mg $IrCl_3$ are dissolved in 20 ml oleylamine, and the mixture is kept at 250℃ for 1h.

Synthesis of OC: First, we prepared Ni@OC-430, then, it was dissolved in 3 M HCl and transferred to Teflon-lined autoclave, keeping at 150℃ for 10h. Finally, the obtained production was washed by water for three times.

Synthesis of Ir/OC-430: The prepared OC was dissolved in 20 ml water, then 10 mg $IrCl_3$ was injected in the mixture, followed by adding 50 mg $NaBH_4$. The solution was stirred for 4h.

Material characterization: The powder XRD patterns of the samples were recorded with an X-ray diffractometer (Japan Rigaku D/MAX-γA) using Cu-Ka radiation (λ=1.54178 Å) with 2θ range of 20–80°. FESEM images were taken on a JEOL JSM-6700M scanning electron microscope. TEM images were collected from Hitachi H-800 transmission electron microscope using an accelerating voltage of 200 kV, and a HRTEM (JEOL-2011) was operated at an accelerating voltage of 200 kV. Inductively coupled plasma-atomic emission spectrometer (ICP-AES) were conducted with an Optima 7300 DV instrument. Raman spectra were obtained using a LabRAM HR Raman spectrometer. The specific surface area was evaluated at 77 K (Autosorb iQ Station 2) using the Brunauer–Emmett–Teller (BET) method applied to the adsorption branch. XPS was performed on an ESCALAB 250 X-ray photoelectron spectrometer using Al Ka radiation. C and N XANES were obtained at soft x-ray magnetic circular dichroism station in national synchrotron radiation laboratory in USTC, Hefei.

Electrochemical measurements: The electrochemical tests were carried out in a three-electrode system on an electrochemical workstation (CHI760E). Typically, 4 mg of catalysts were dispersed in 1 mL ethanol. Then, 30 μL Nafion solution (Sigma Aldrich, 5 wt %) was added into the solution and subsequently sonicated for 1h to form a homogeneous ink. 5 μL of the dispersion was loaded onto a glassy carbon electrode with 3 mm diameter. A graphite rod and an Ag/AgCl electrode were used as the counter electrode and reference electrode, respectively. Linear sweep voltammetry was conducted in N_2-saturated 0.5 M H_2SO_4 and 1 M KOH solutions with a scan rate of 2 mV s^{-1}. Cyclic

voltammetry (CV) was conducted in both acidic and basic media at a sweep rate of 50 mV s^{-1}. All the potentials were quoted against a reversible hydrogen electrode (RHE).

DFT calculation details: The DFT calculations were performed using the Vienna Ab Initio Simulation Package (VASP), and the generalized gradient approximation (GGA) of Perdew-Becke-Ernzerhof (PBE) is used for the exchange-correlation functional. The cut-off energy was set to 450 eV for the plane-wave expansion of the electronic wave function. All structures were optimized with a convergence criterion of 1×10^{-5} eV for the energy and 0.01 eV/Å for the forces. The k-point mesh of 5 × 5 × 1 was used to represent the Brillouin zone. The free energy of the adsorbed state was calculated as $\Delta G_{H^*} = \Delta E(H^*) + \Delta ZPE - T\Delta S$, where $\Delta E(H^*)$ is the hydrogen absorption energy, ΔZPE is the difference in zero-point energy between the adsorbed hydrogen and hydrogen in the gas phase. And ΔS is the entropy difference between the adsorbed state and the gas phase. As the contribution from the vibrational entropy of H in the adsorbed state is negligibly small, the entropy of hydrogen adsorption is $\Delta SH \approx -\frac{1}{2}S_{H2}$, where S_{H2} is the entropy of H_2 in the gas phase at the standard conditions. Thus, the Gibbs free energy with the overall corrections is taken as $\Delta G_{H^*} = \Delta E_{H^*} + 0.24$ eV.

Supporting figures

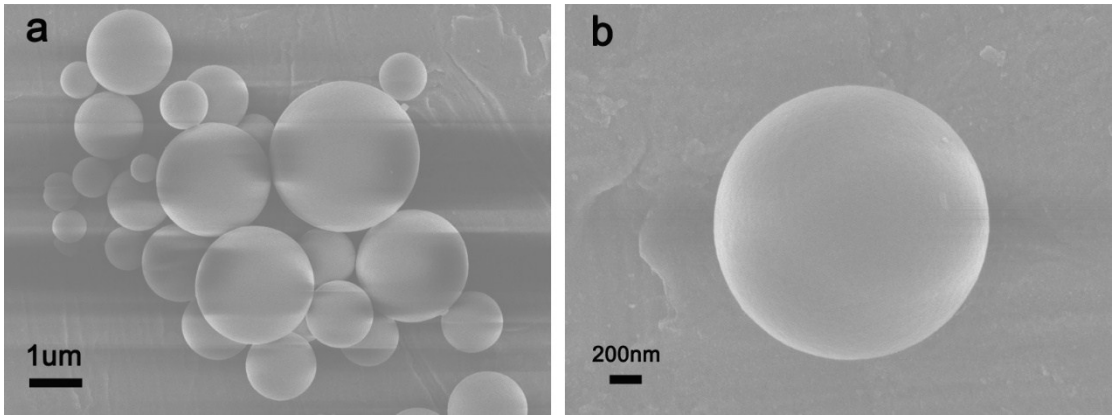

Figure S1. a), b) The SEM of Ni-btc precursor.

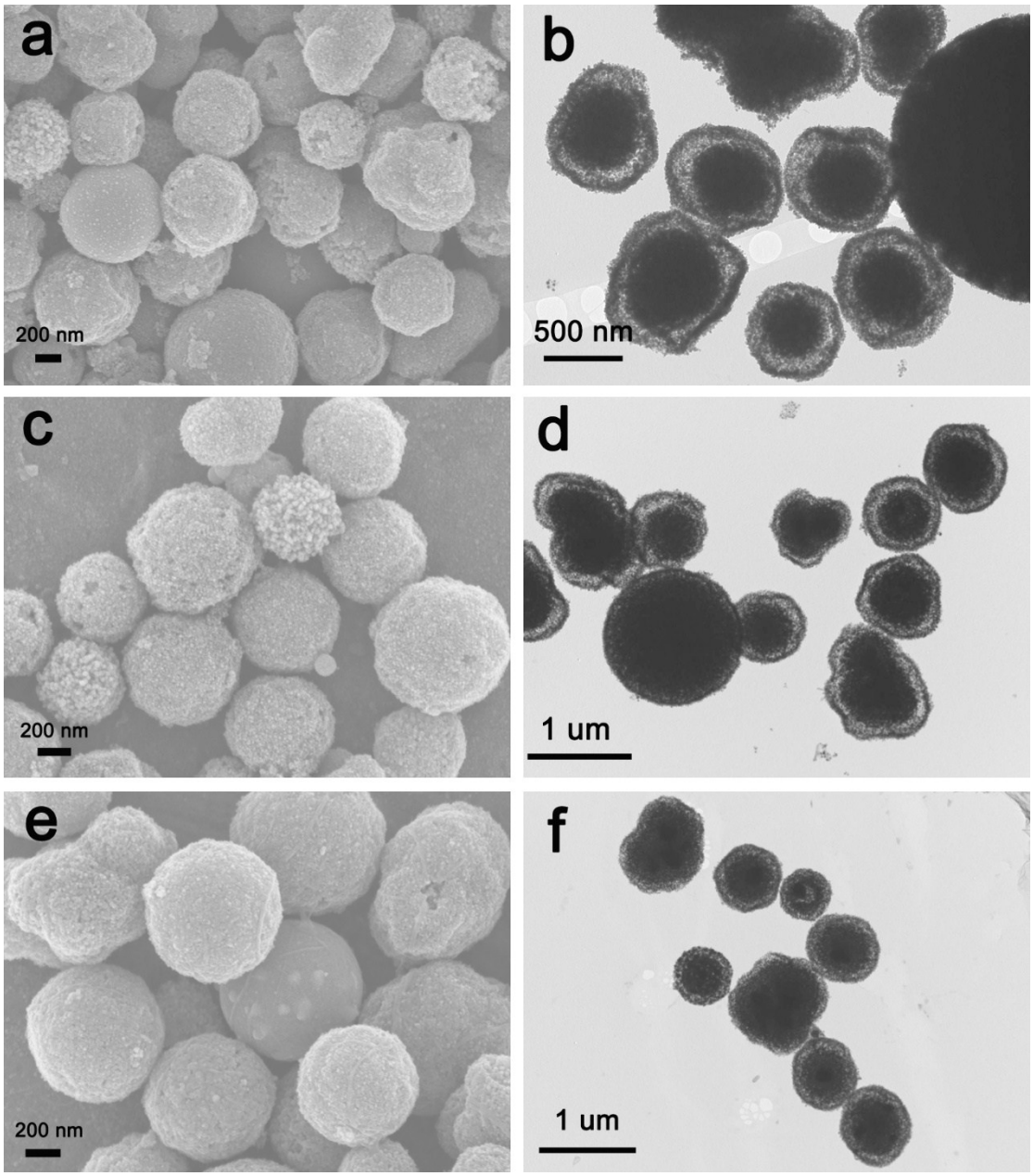

Figure S2. a-b) SEM and TEM images of IrNi@OC-500. c-d) SEM and TEM images of IrNi@OC-600. e-f) SEM and TEM images of IrNi@OC-700.

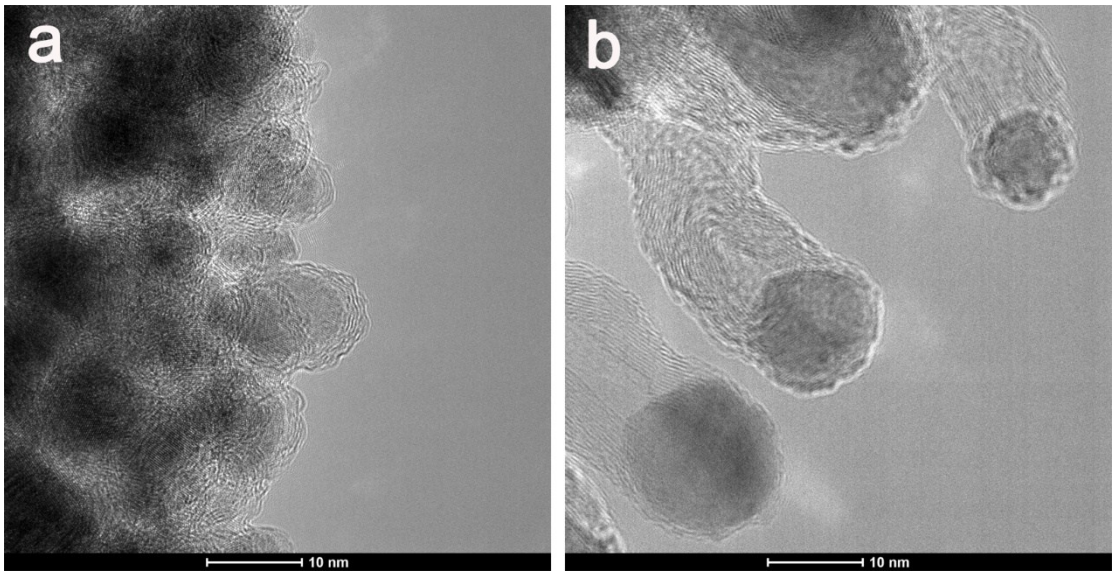

Figure S3. a) HRTEM image of IrNi@OC-430. b) HRTEM image of Ni@OC-430.

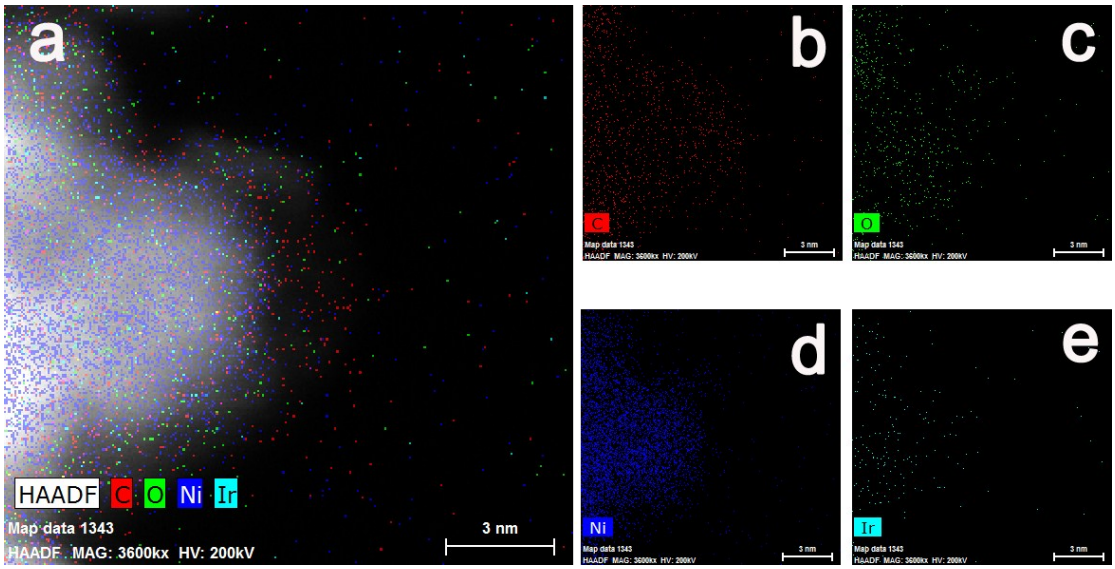

Figure S4. The magnified mapping results of the ultrafine nanoparticle on surface of IrNi@OC-430. C and O elements distribute on the out shell, and Ir, Ni elements are encapsulated.

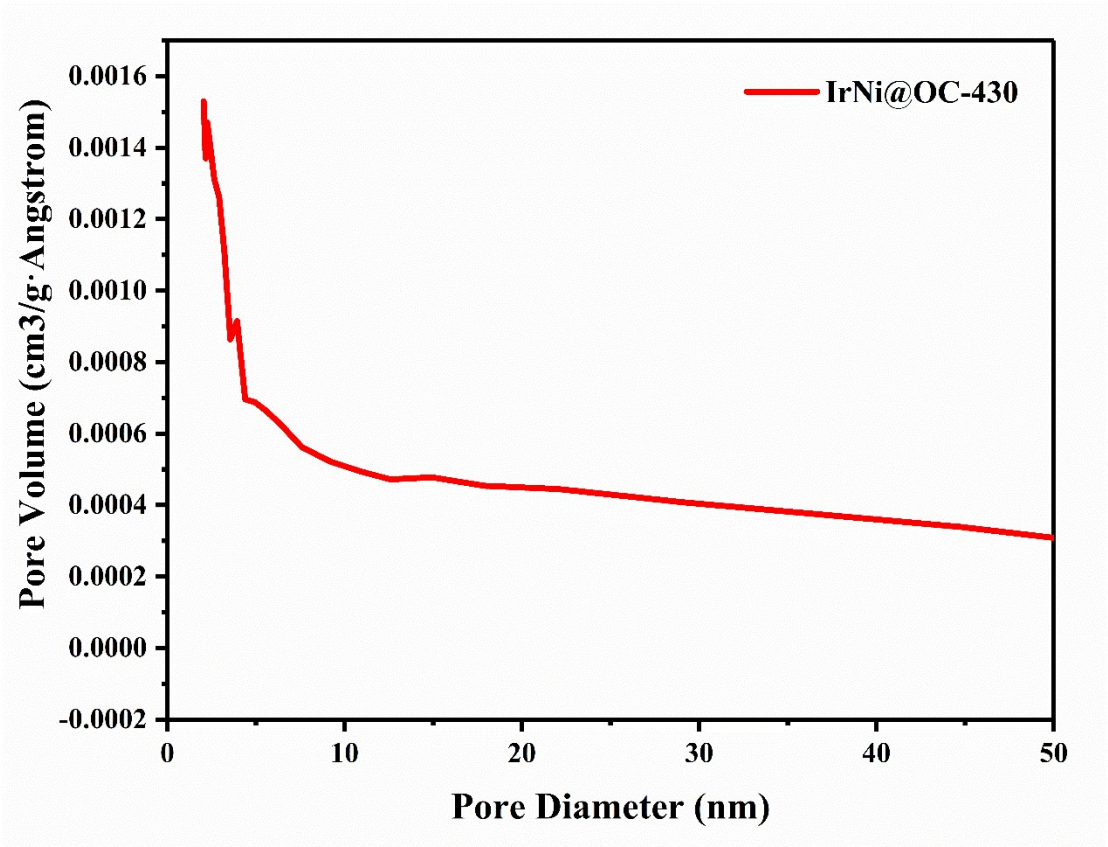

Figure S5. The pore size distribution of IrNi@OC-430 from BET results.

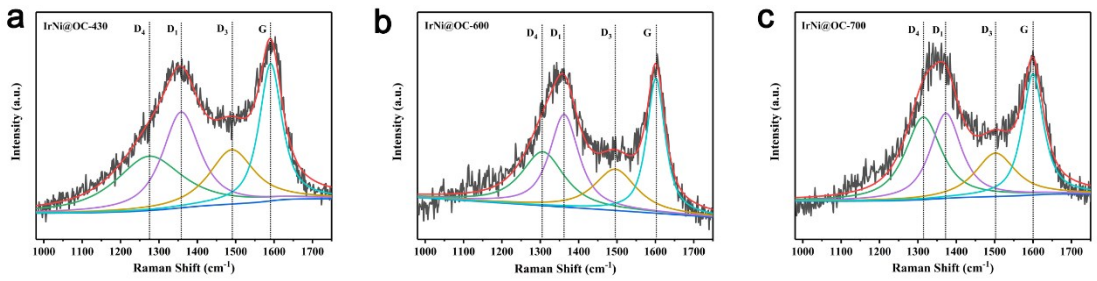

Figure S6. Raman spectra of a) IrNi@OC-430, b) IrNi@OC-600, c) IrNi@OC-700. The spectrum of each sample can be divided into four peaks D_1, D_3, D_4, G.

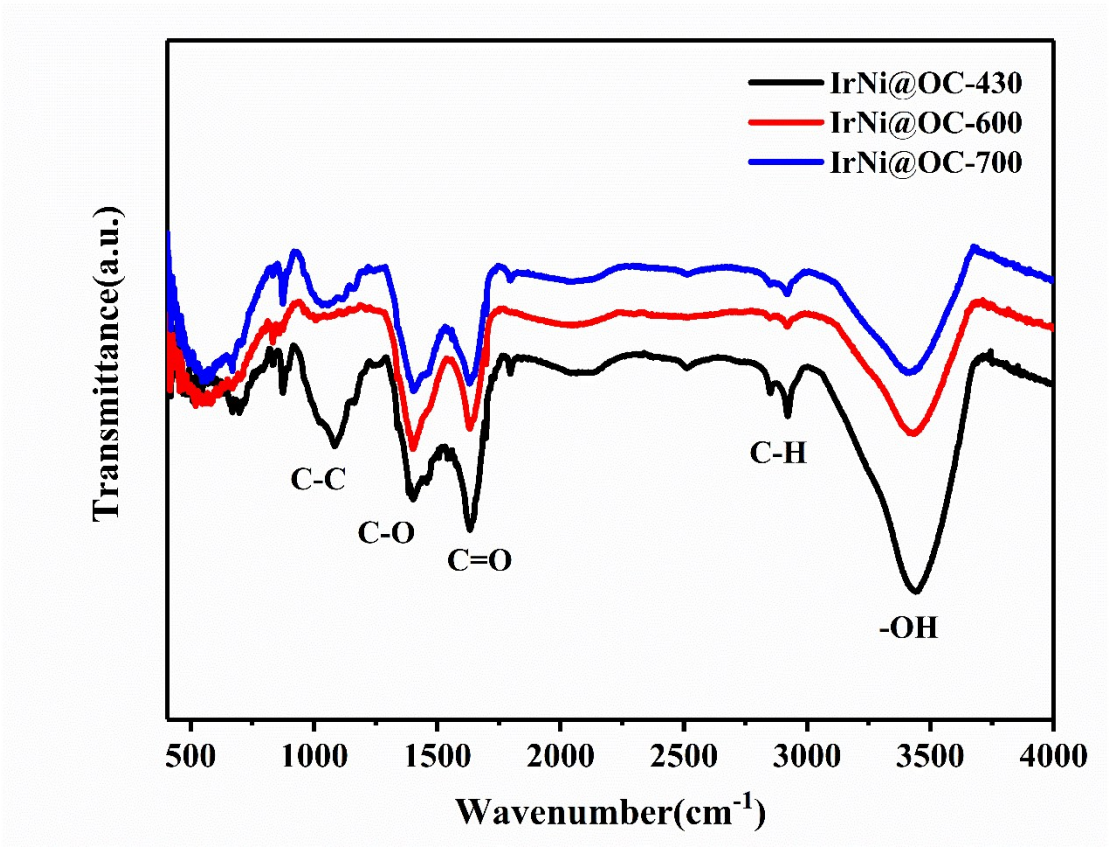

Figure S7. IR spectra of IrNi@OC-430, 600,700, respectively.

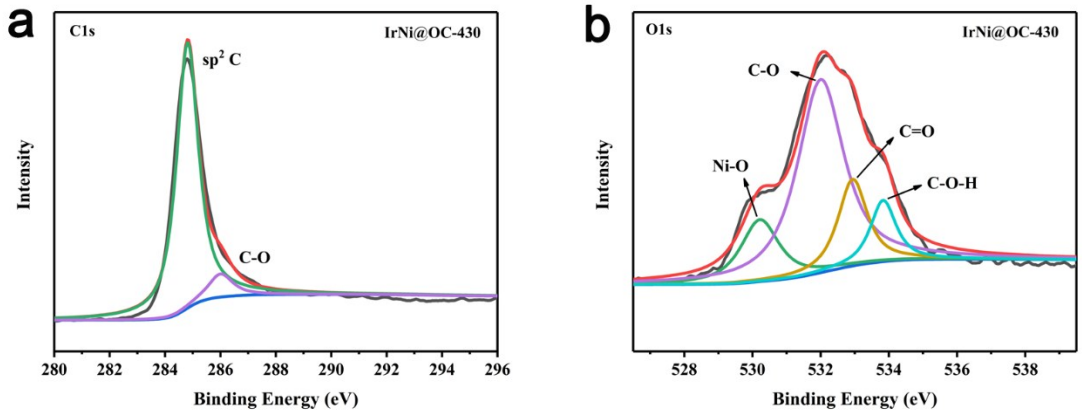

Figure S8. a) C 1s and b) O 1s spectra of IrNi@OC-430.

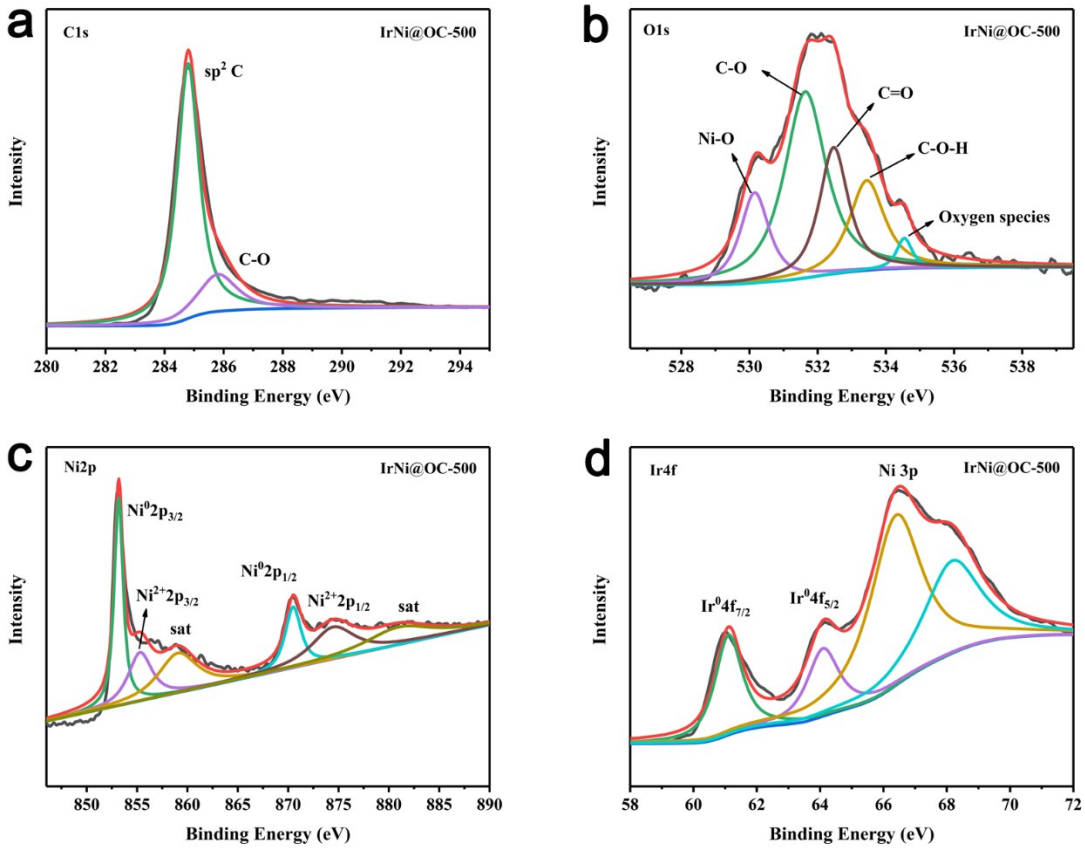

Figure S9. a-d) C 1s, O 1s, Ni 2p, Ir 4f xps spectra of IrNi@OC-500, respectively.

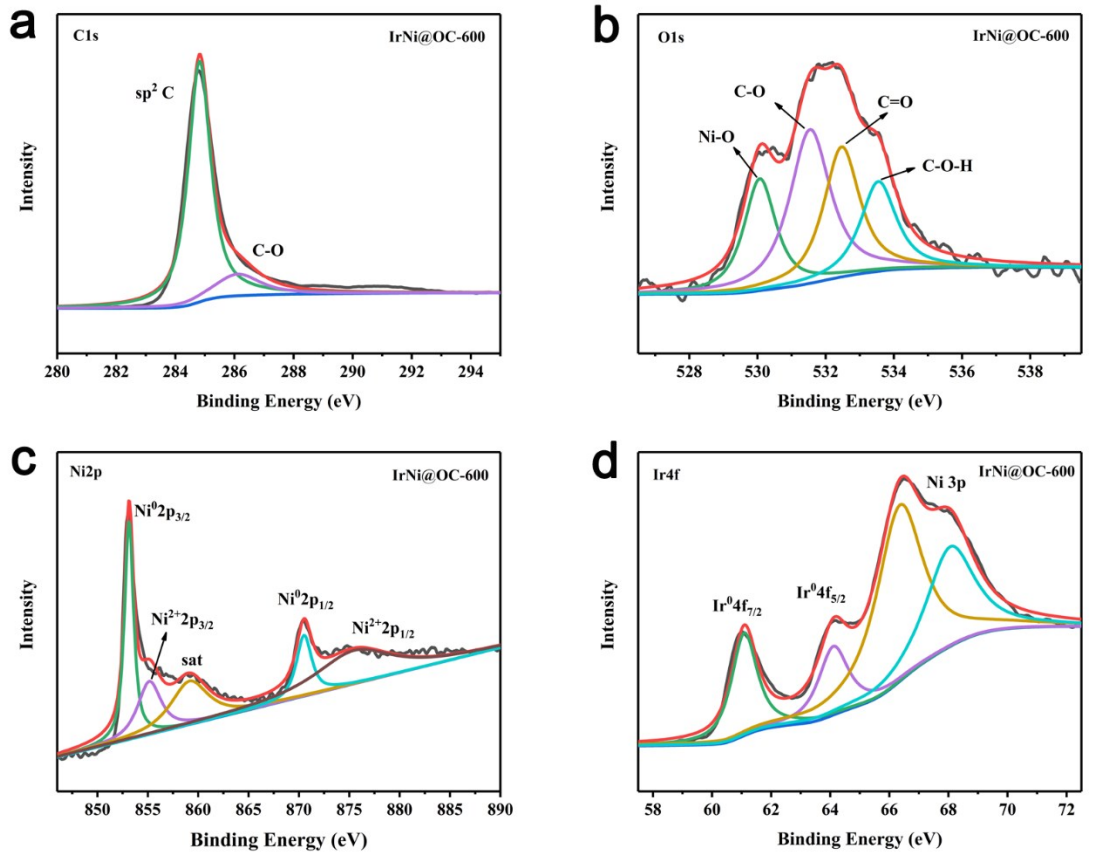

Figure S10. (a-d) C 1s, O 1s, Ni 2p, Ir 4f of IrNi@OC-600, respectively.

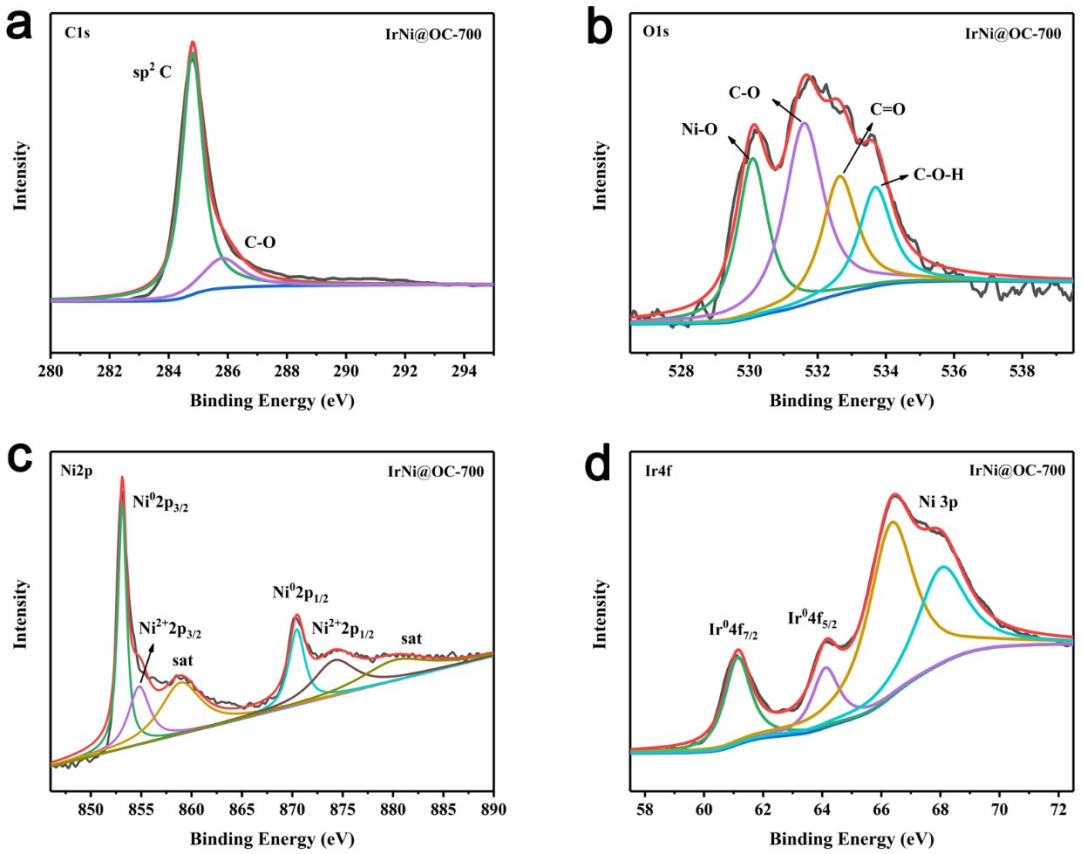

Figure S11. (a-d) C 1s, O 1s, Ni 2p, Ir 4f of IrNi@OC-600, respectively.

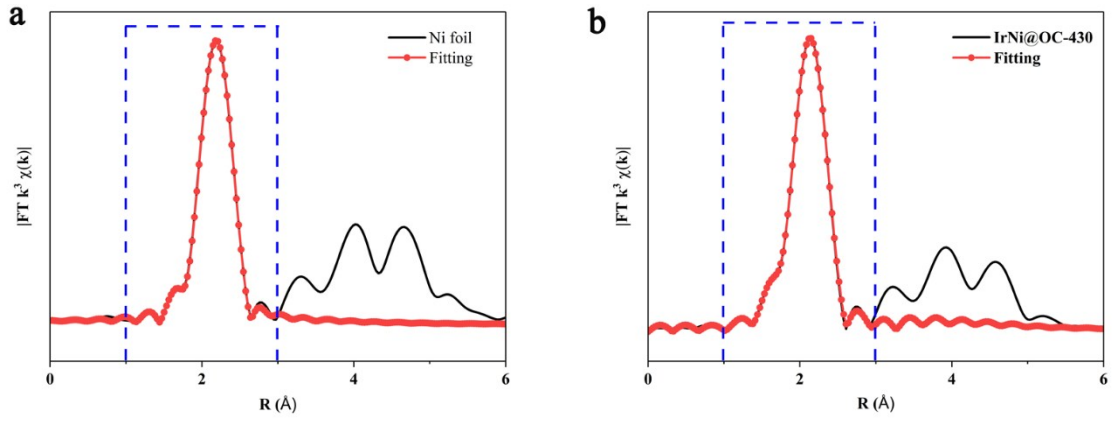

Figure 12. *R* space and inverse FT-EXAFS fitting results of Ni K-edge. a) Ni foil. b) IrNi@OC-430.

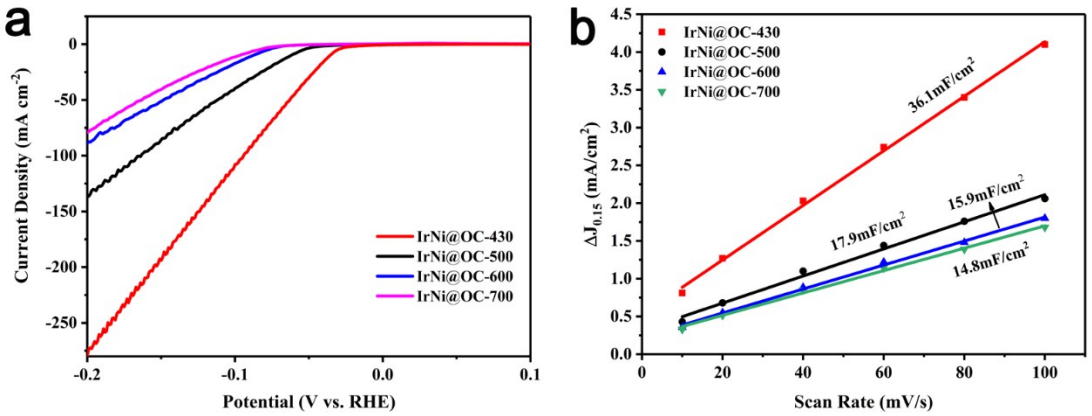

Figure S13. a) LSV polarization curves of IrNi@OC-430, 500, 600, 700 in 0.5 M H_2SO_4. b) Double-layer capacitance (C_{dl}) value of IrNi@OC-430, 500, 600, 700 in 0.5 M H_2SO_4.

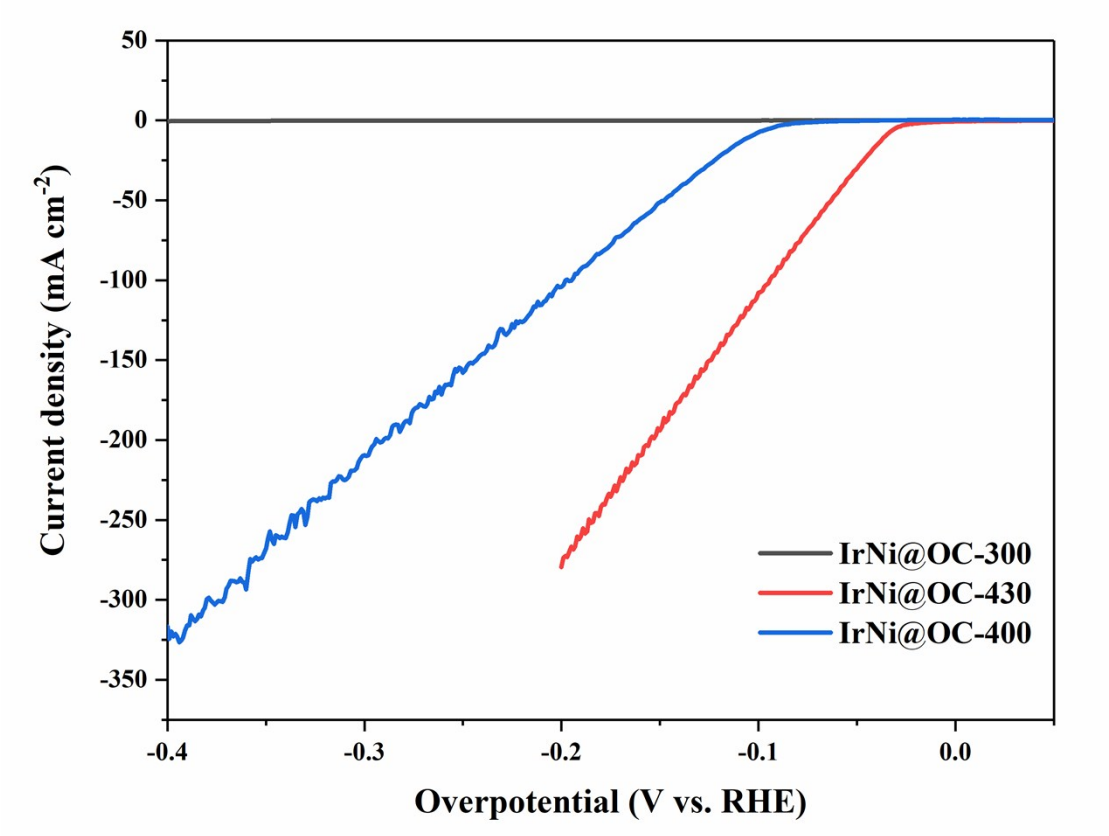

Figure S14. The HER performance of IrNi@OC-300, 400, 430 in 0.5 M H_2SO_4.

Figure S15. Digital photo of the light blue solution after 0.5 M H2SO4 etching overnight.

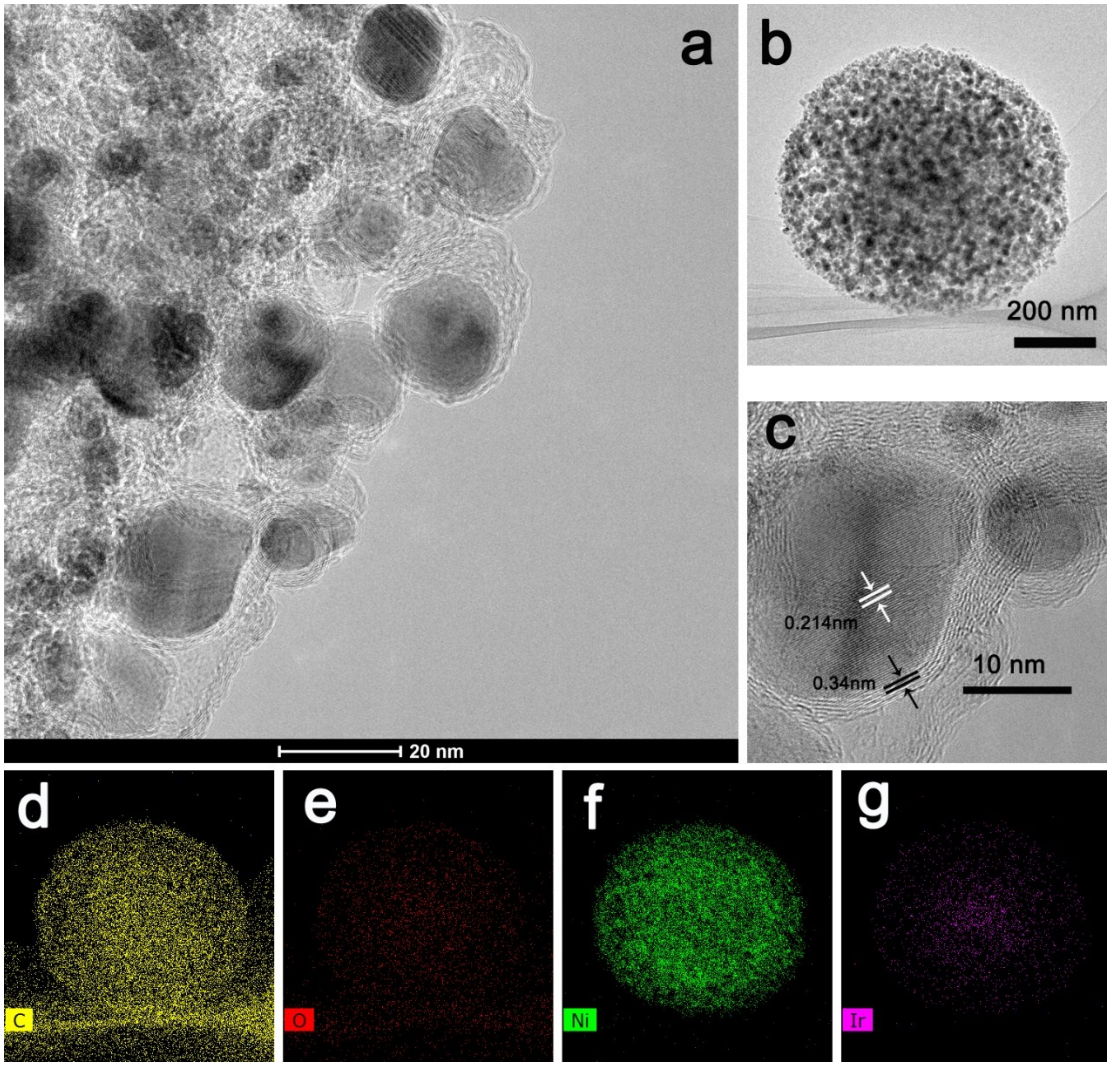

Figure S16. The HRTEM images of IrNi@OC-430 after 0.5 M H_2SO_4 etched overnight. a) HRTEM image of IrNi@OC-430 after acid etched. The results reveal that after acid treated, the IrNi alloy encapsulated in graphene completely still maintain the initial structure, and the hollow carbon cages suggest that some unstable metal nanoparticles are etched. b) TEM image of IrNi@OC-430 after acid etched. The obvious pores left in the sphere after acid treated reveal that many unstable metal nanoparticles are etched. c) The magnified HRTEM image. The measured distance of lattice fringe space of metal nanoparticle and shell is 0.214 nm and 0.34 nm, respectively, which indeed demonstrate that the metal core is IrNi alloy and the outside shell is graphene layers. d-g) Elements mapping of C, O, Ni, Ir of IrNi@OC-430 after acid etched.

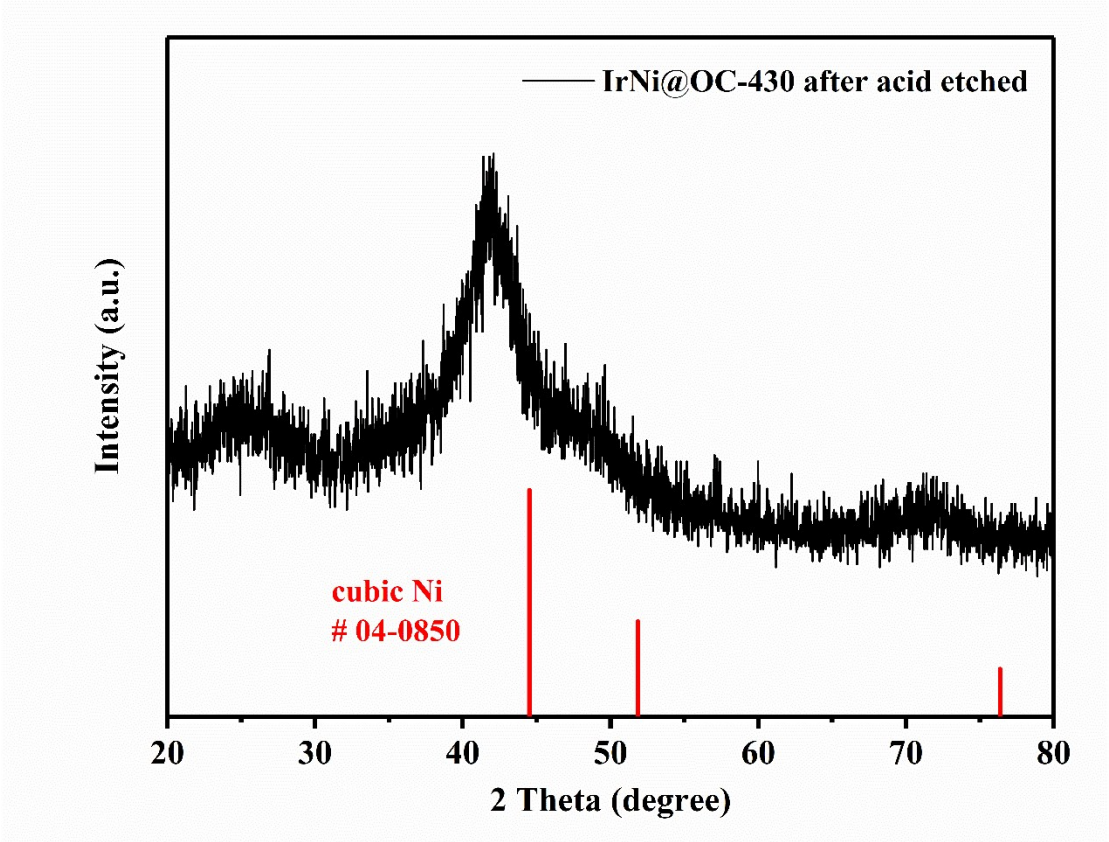

Figure S17. XRD pattern of IrNi@OC-430 after 0.5 M H_2SO_4 etched overnight. The results show the peaks correspond to pure Ni with a little left shift.

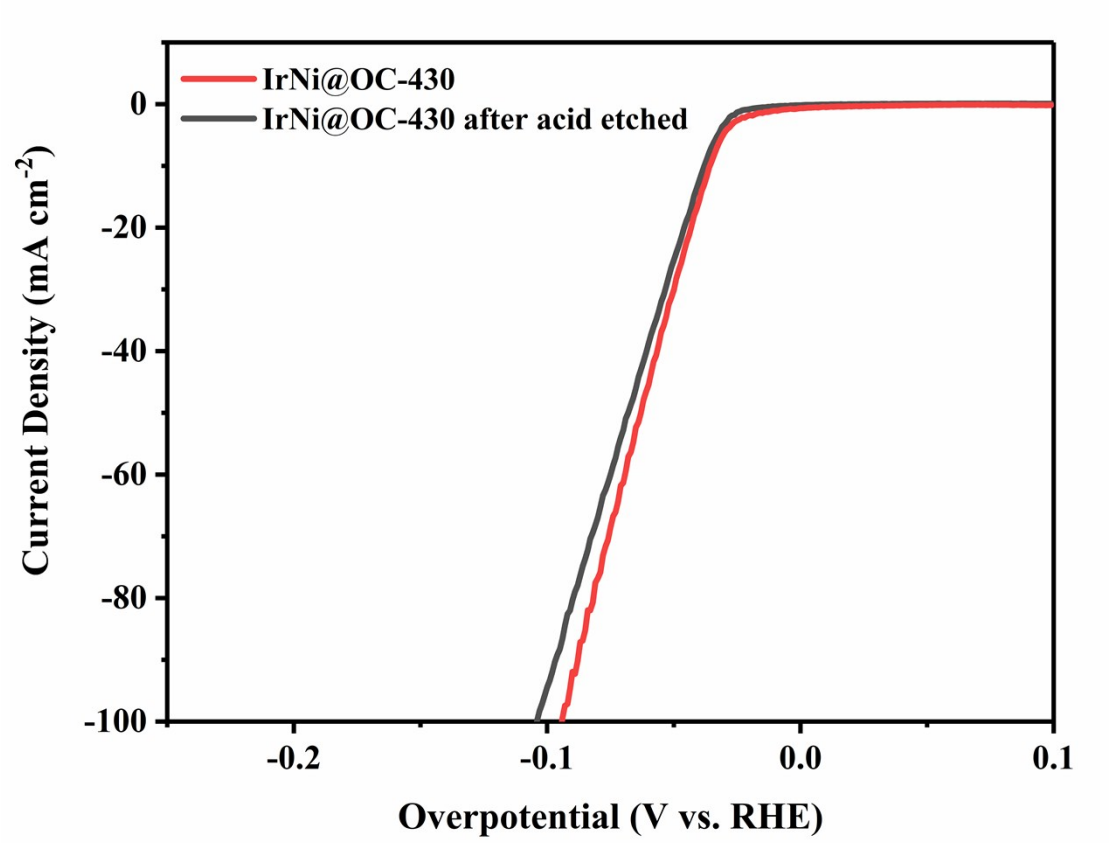

Figure S18. HER performance of IrNi@OC-430 before and after acid etched in 0.5 M H_2SO_4 electrolyte.

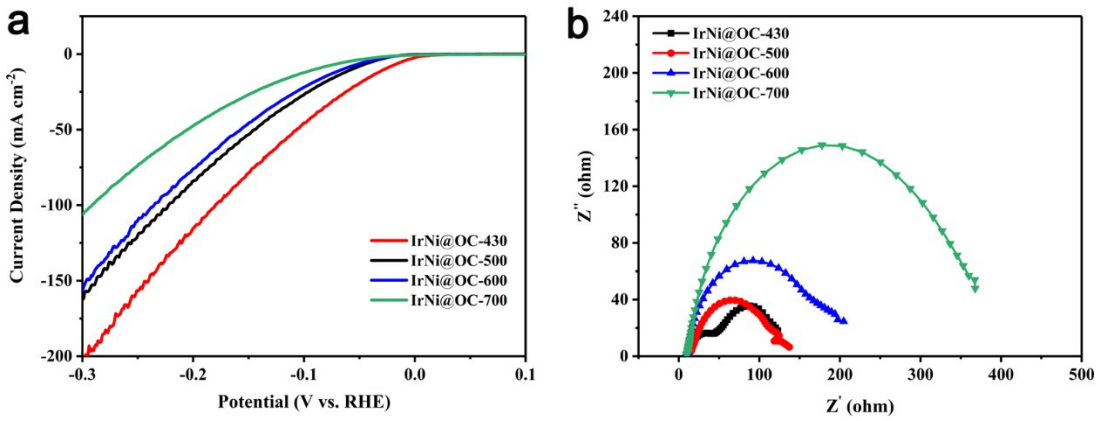

Figure S19. a) LSV polarization curves of IrNi@OC-430, 500, 600, 700 in 1 M KOH. b) Double-layer capacitance (C_{dl}) value of IrNi@OC-430, 500, 600, 700 in 1 M KOH.

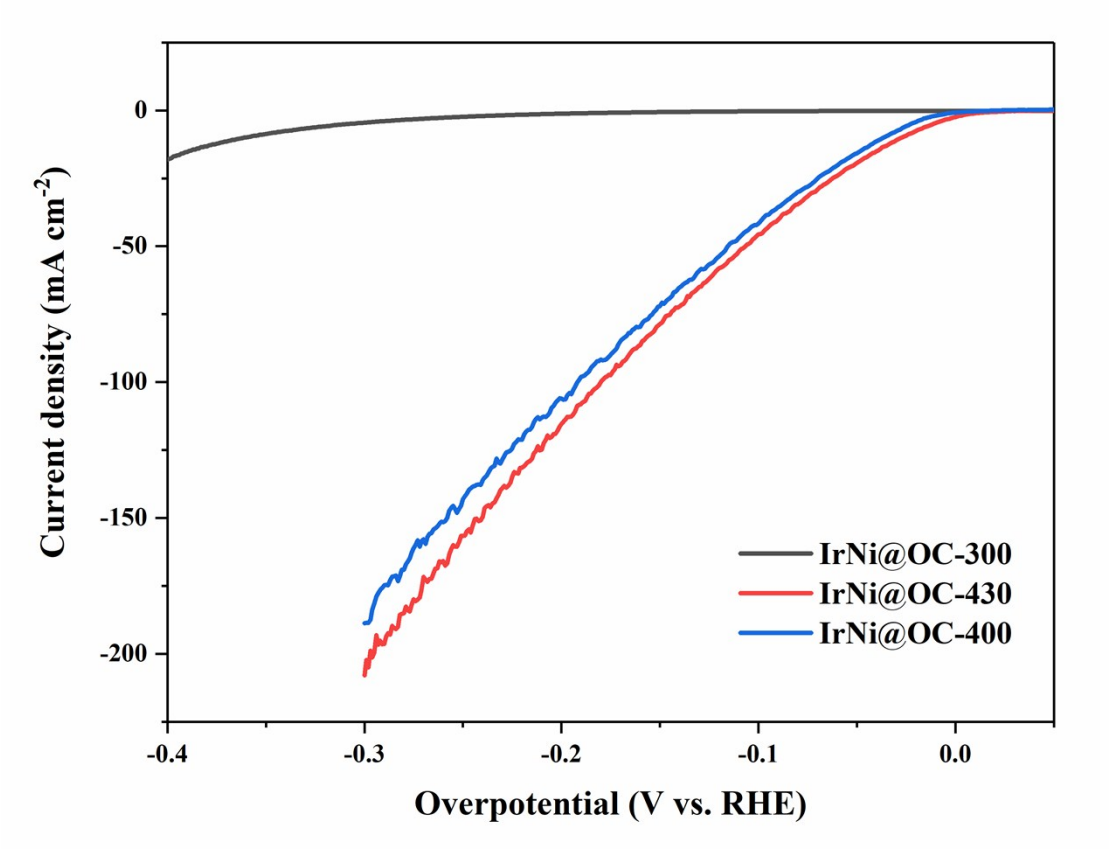

Figure 20. The HER performance of IrNi@OC-300, 400, 430 in 1 M KOH.

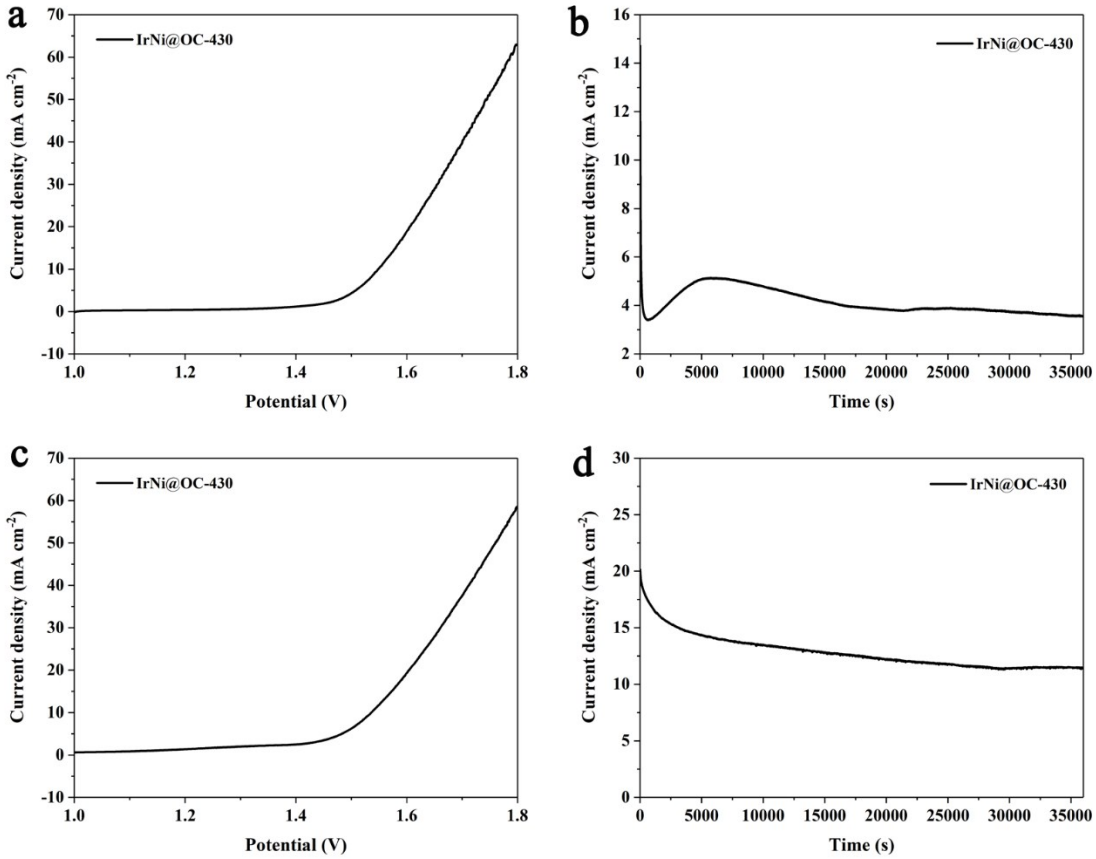

Figure 21. a) LSV polarization curve b) chronoamperometry test of water splitting in 0.5 M

H_2SO_4. c) LSV polarization curve d) chronoamperometry test of water splitting in 1 M KOH.

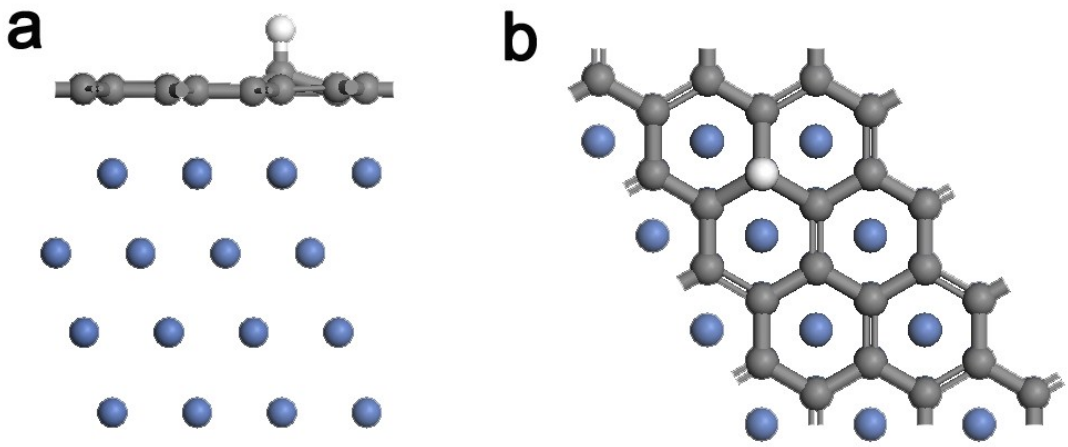

Figure S22. a) side and b) top view of the optimized structure of Ni@C with an adsorbed H atom.

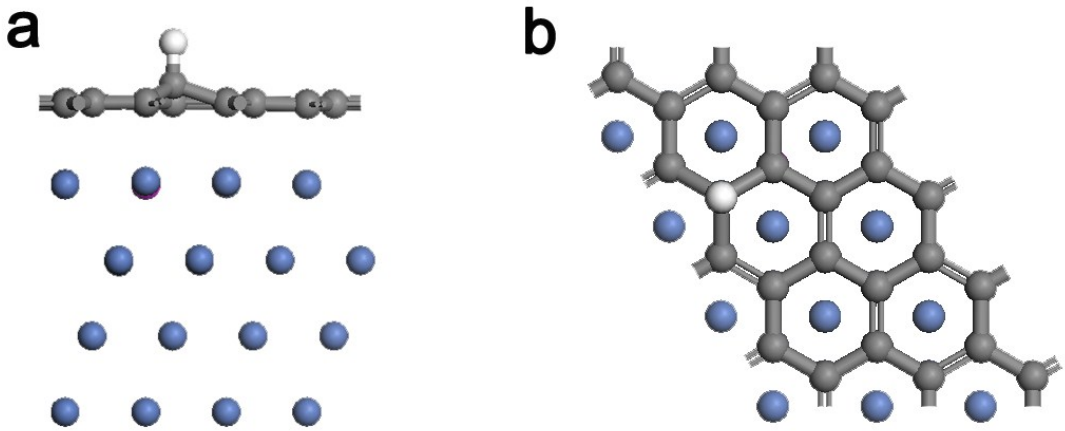

Figure S23. a) side and b) top view of the optimized structure of IrNi@C with an adsorbed H atom.

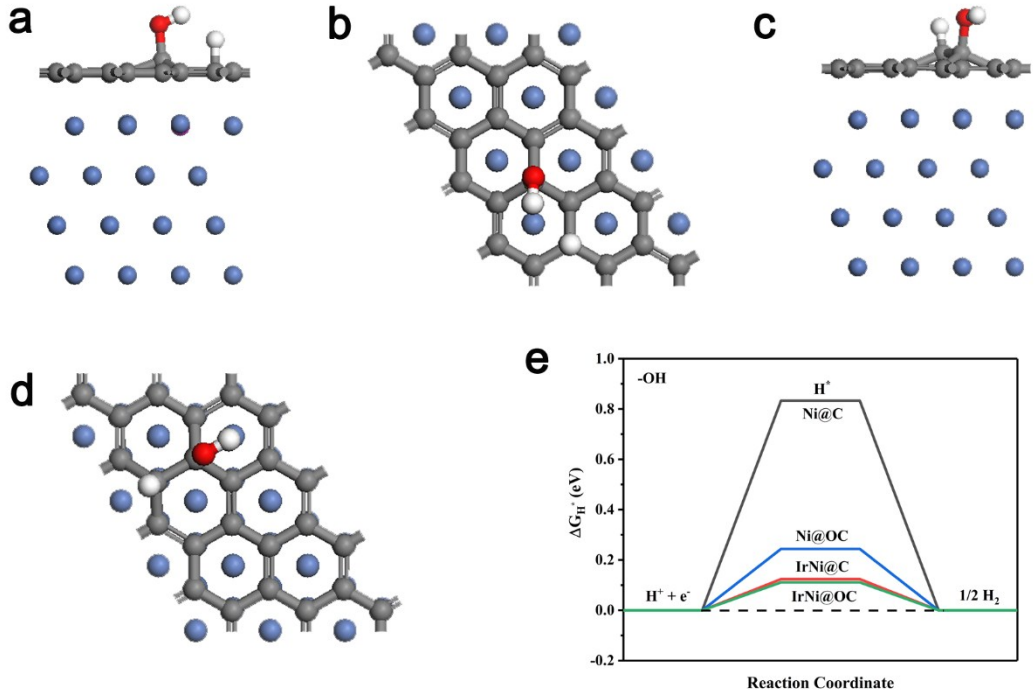

Figure S24. a-b) Side and top view of the optimized structure of IrNi@OC-430 (here the O species is -OH) with an adsorbed H atom. c-d) Side and top view of the optimized structure of Ni@OC (-OH) with an adsorbed H atom as comparison. e) Gibbs free energy (ΔG_{H^*}) diagram of Ni@C, Ni@OC, IrNi@C, and IrNi@OC.

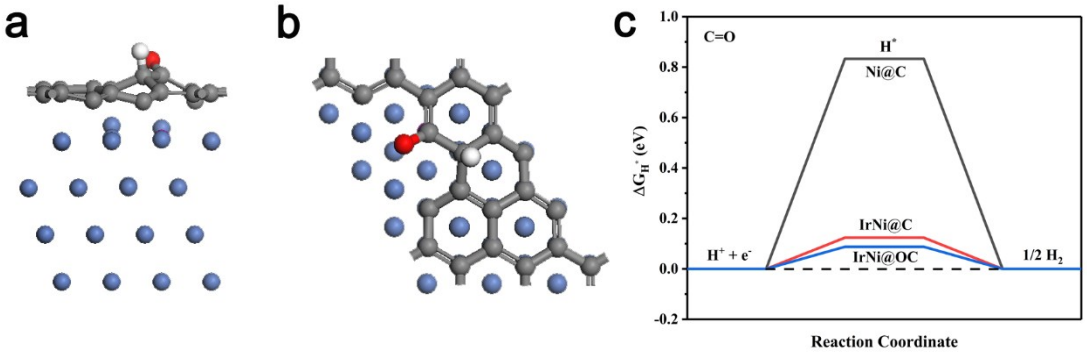

Figure 25. a-b) Side and top view of the optimized structure of IrNi@OC (O species is C=O) with an adsorbed H atom. c) Free energy (ΔG_{H^*}) diagram of Ni@C, IrNi@C, and IrNi@OC.

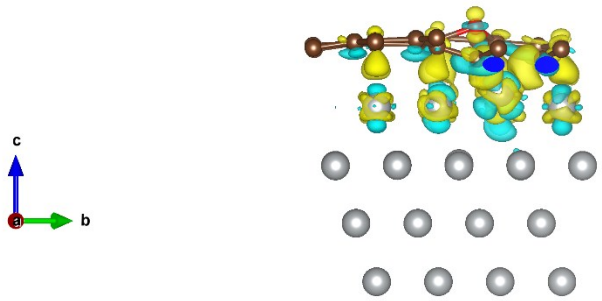

Figure S26. The side view of charge-density difference of IrNi@OC (pyran O). The isosurface value of the color region is 0.01 eÅ^{-3}. The yellow and cyan regions refer to increased and decreased charge distributions, respectively.

Table S1. The content of O in IrNi@OC-T (T= 430, 500, 600, 700) by XPS results.

Sample	IrNi@OC-430	IrNi@OC-500	IrNi@OC-600	IrNi@OC-700
O (atom%)	11.77	5.99	4.74	4.35

Table S2. Curve fitting results of Ni K-edge EXAFS of Ni foil and IrNi@OC-430.

Samples	Shell	CN	R(Å)	σ^2(10^{-3}Å)	R factor
Ni foil	Ni-Ni	12	2.48	6.0	0.00189
IrNi@OC-430	Ni-Ni	8.5	2.49	6.8	0.00127
	Ni-Ir	1.6	2.54	18	
	Ni-O	1.7	2.13	14	

Table S3. The HER catalytic performance of reported catalysts.

Catalyst	Loading amount (mg cm^{-2})	Electrolyte	Overpotential at 10 mA cm^{-2} (mV)	Reference
IrNi@OC-430	0.285	0.5 M H_2SO_4	35	**This work**
		1.0 M KOH	27	
Ni@NC-800	0.31	1.0 M KOH	205	Adv. Mater. 2017, 1605957

NiCu@C	0.384	0.5 M H_2SO_4 1.0 M KOH	48 74	Adv. Energy Mater.2018, 8, 1701759
MoC_x	0.8	0.5 M H_2SO_4 1.0 M KOH	142 151	Nat. Commun. 2015, 6, 7512
RuP_2@NPC	1	0.5 M H_2SO_4 1.0 M KOH	38 52	Angew. Chem. Int. Ed. 2017, 56, 1
Ru/C_3N_4/C	0.204	0.5 M H_2SO_4 1.0 M KOH	69 79	J. Am. Chem. Soc.2016, 138, 16174
Co@N-CNTs@rGO	-	0.5 M H_2SO_4 1.0 M KOH	87 108	Adv. Mater. 2018, 30, 1802011
Rh-MoS_2	0.309	0.5 M H_2SO_4	47	Adv. Funct. Mater. 2017, 27, 1700359
W-SAC	0.408	0.1 M KOH	85	Adv.Mater. 2018, 30, 1800396
CoN_x/C	2.0	1.0 M KOH	170	Nat. Commun. 2015, 6, 7992